^{68}Ga-PSMA-11 PET/CT in Newly Diagnosed Carcinoma of the Prostate: Correlation of Intraprostatic PSMA Uptake with Several Clinical Parameters

Stefan A. Koerber[1–3], Maximilian T. Utzinger[4], Clemens Kratochwil[4,5], Claudia Kesch[6], Matthias F. Haefner[1–3], Sonja Katayama[1–3], Walter Mier[4], Andrei H. Iagaru[7], Klaus Herfarth[1–3], Uwe Haberkorn[4,5], Juergen Debus[1–3], and Frederik L. Giesel[4,5,8]

[1]Department of Radiation Oncology, University Hospital Heidelberg, Heidelberg, Germany; [2]Clinical Cooperation Unit Radiation Oncology, German Cancer Research Center (DKFZ), Heidelberg, Germany; [3]National Center of Radiation Oncology (NCRO), Heidelberg Institute of Radiation Oncology (HIRO), Heidelberg, Germany; [4]Department of Nuclear Medicine, University Hospital Heidelberg, Heidelberg, Germany; [5]Clinical Cooperation Unit Nuclear Medicine, German Cancer Research Center (DKFZ), Heidelberg, Germany; [6]Department of Urology, University Hospital Heidelberg, Heidelberg, Germany; [7]Division of Nuclear Medicine and Molecular Imaging, Stanford Health Care, Stanford, California; and [8]German Cancer Consortium (DKTK), Heidelberg, Germany

^{68}Ga-prostate-specific membrane antigen (PSMA) PET/CT is a promising diagnostic tool for patients with prostate cancer. Our study evaluates SUVs in benign prostate tissue and malignant, intraprostatic tumor lesions and correlates results with several clinical parameters. **Methods:** One hundred four men with newly diagnosed prostate carcinoma and no previous therapy were included in this study. SUV_{max} was measured and correlated with biopsy findings and MRI. Afterward, data were compared with current prostate-specific antigen (PSA) values, Gleason score (GS), and d'Amico risk classification. **Results:** In this investigation a mean SUV_{max} of 1.88 ± 0.44 in healthy prostate tissue compared with 10.77 ± 8.45 in malignant prostate lesions ($P < 0.001$) was observed. Patients with higher PSA, higher GS, and higher d'Amico risk score had statistically significant higher PSMA uptake on PET/CT ($P < 0.001$ each). **Conclusion:** PSMA PET/CT is well suited for detecting the intraprostatic malignant lesion in patients with newly diagnosed prostate cancer. Our findings indicate a significant correlation of PSMA uptake with PSA, GS, and risk classification according to the d'Amico scale.

Key Words: prostate cancer; PSMA PET/CT; SUV; Gleason score; radiotherapy

J Nucl Med 2017; 58:1943–1948
DOI: 10.2967/jnumed.117.190314

The glycosylated transmembrane protein prostate-specific membrane antigen (PSMA) has higher expression in prostate cancer cells than nonmalignant prostate tissue (*1,2*). In the last years, several PSMA-targeting radiopharmaceuticals have been developed for diagnostic or therapeutic use in prostate cancer. One of them, ^{68}Ga-labeled PSMA-HBED-CC (PSMA-11), showed promising results in first in vivo studies (*3–5*) and emerged as the most frequently used PSMA-targeting tracer up to date. Currently, ^{68}Ga-PSMA PET/CT offers excellent diagnosis for prostate cancer in various clinical scenarios. Although modern MRI techniques such as multiparametric MRI are likely to improve the detection of clinically significant cancer, there are still conflicting results, for example, concerning the role as a prebiopsy diagnostic tool (*6,7*). With a high sensitivity and specificity of up to 70% and 100%, PSMA PET/CT is well suited for assessing the extent of primary prostate cancer or the detection of lymph node metastases and proved to be superior to standard routine imaging (*8,9*). Even compared with ^{18}F-choline PET/CT, this modern diagnostic tool has high detection rates also in patients with low prostate-specific antigen (PSA) values and negative choline imaging (*10*). Although prospective, validating data are still missing, some retrospective studies reported on numerous changes in TNM stage or treatment management after ^{68}Ga-PSMA PET/CT examination (*11–13*). One study with 57 patients performed by Sterzing et al. observed a therapy change in 50.8% of all cases (*12*).

There is a positive correlation between PSMA expression and Gleason score (GS). Several preclinical studies demonstrated that high PSMA expression was significantly correlated with higher GS (*14,15*). Perner et al. used tumor samples from 450 prostate cancer patients and compared PSMA expression with different clinical parameters. The authors concluded that high immunohistochemical PSMA expression in primary tumor is able to predict disease outcome independently (*16*). To our knowledge, there is only 1, larger study with robust in vivo data yet (*17*). Most of the published studies were based on tumor samples received from surgery or biopsy.

Therefore, the aim of this study was to evaluate differences of SUV measurements in healthy prostate tissue versus malignant prostate lesions based on a high proportion of MRI/transrectal ultrasound (TRUS)–fusion biopsy results in a large group of untreated patients with newly diagnosed prostate carcinoma undergoing PSMA PET/CT. In addition, we performed correlations for SUV measurements and clinical parameters such as GS and d'Amico scale.

Received Jan. 19, 2017; revision accepted May 4, 2017.
For correspondence or reprints contact: Frederik L. Giesel, Department of Nuclear Medicine, University Hospital Heidelberg, Im Neuenheimer Feld 400, 69120 Heidelberg, Germany.
E-mail: frederik@egiesel.com
Published online Jun. 15, 2017.

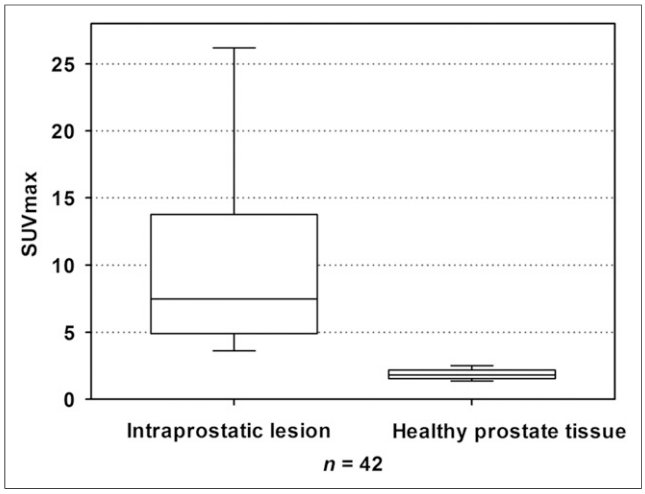

FIGURE 1. Box plot of SUV_{max} from malignant (left) and normal (right) intraprostatic tissue.

MATERIALS AND METHODS

Patient Characteristics

This study was approved by the local ethics committee (S-595/2016). Between June 2011 and February 2017, PSMA PET/CT was performed for 177 consecutive men with newly diagnosed, treatment-naïve, and biopsy-proven prostate cancer in the Department of Nuclear Medicine, University Hospital Heidelberg. Forty-eight patients received androgen deprivation at the time of PSMA PET/CT. These men were excluded from analysis because of possible effects of androgens on PSMA uptake (*18–20*). Because of an interval different from 60 ± 10 min between injection of the tracer and acquisition, another 20 patients were not included in the study. We chose this interval in clinical routine for better interindividual comparability. From the remaining 109 men, sufficient clinical data were available for a total of 104 patients included in this analysis. All 104 patients underwent biopsy (48.1% multiparametric MRI/TRUS-fusion biopsy, 51.9% TRUS-guided biopsy) before imaging.

For 67 patients (64.42%), an additional multiparametric MRI scan of the prostate was obtained—in most cases within the preparation for biopsy. Twenty-eight men (26.92%) underwent surgery (radical prostatectomy) after PSMA PET/CT. Only patients (n = 42) with additional MRI scans and histopathologic data from surgery and clearly delineated, healthy tissue in the prostate were used for intraprostatic SUV comparison between normal and malignant prostate tissue to avoid incorrect measurements. For correlation with clinical parameters, all patients (n = 104) were included except 1 patient with missing current PSA value.

PSMA PET/CT Imaging

The synthesis of ^{68}Ga-PSMA-11 (median, 200.5 MBq; range, 92–338 MBq) was done as described by Eder et al. (*21*). After intravenous injection of the tracer (60 ± 10 min), PET/CT imaging was performed with a Biograph PET/CT 6 (n = 59) and mCT Flow (n = 45) scanner (Siemens).

An unenhanced CT scan (130 keV, 80 mAs; CareDose) was obtained for attenuation correction of the PET scan. Static emission scans, corrected for dead time, scatter, and decay, were acquired from the vertex to the mid thighs, requiring 8 bed positions with 3 min per bed position. The images were reconstructed using an ordered-subset expectation maximization algorithm with 4 iterations and 8 subsets and gaussian filtering to an in-plane spatial resolution of 5 mm in full width at half maximum. The CT scan was reconstructed with a B30 or B31 kernel to a slice thickness of 5 mm with an increment of 2.5 mm. For comparability of SUVs between the Biograph 6 and mCT Flow, we used the equivalence SUV provided by Biograph mCT-Flow–related software syngo.

PSMA PET/CT images were evaluated by 2 board-certified nuclear medicine physicians and 1 board-certified radiooncologist by consensus. According to clinical routine at our institution, physicians were not masked to patient characteristic. For imaging evaluation, SUV_{max} was measured in gluteal muscle, intraprostatic lesion, and for patients with available MRI and pathology report in healthy prostate tissue. For calculation of the SUV_{max} of intraprostatic lesions, we drew a volume of interest around the area with the highest GS, indicated by biopsy results. A volume of interest of 10 ± 0.15 cm^3 for gluteal muscle and 1 ± 0.06 cm^3 for healthy prostate tissue was chosen.

TABLE 1
Patient Characteristics

Characteristic	All patients (n = 104)
Median age (y)	67.4 (range, 38–84)
Clinical tumor stage	
T1a	—
T1b	—
T1c	39
T2a	1
T2b	1
T2c	25
T3a	7
T3b	26
T4	5
N0	72
N1	32
M0	82
M1a	3
M1b	17
M1c	2
GS (biopsy)	
6	15
7a	24
7b	16
8	19
9	26
10	4
Current PSA	
<10 ng/mL	35
10–20 ng/mL	30
>20 ng/mL	38
Unknown	1
d'Amico score (21)	
Low risk	6
Intermediate risk	17
High risk	81

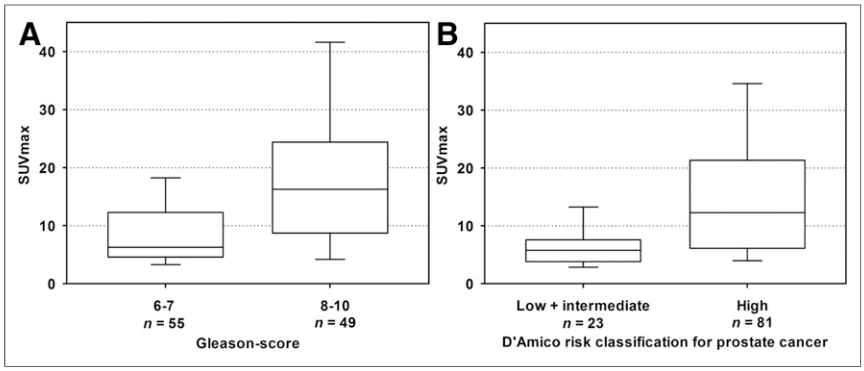

FIGURE 2. Box plot of SUV_{max} according to GS in biopsy (A) and d'Amico classification (B).

Healthy prostate tissue was selected in correlation with MRI and, if available, the pathology report after subsequent prostatectomy. For our analysis we chose SUV_{max}, because it offers a greater reproducibility than SUV_{mean}, as it does not depend on the size of the volume of interest (*3*).

Statistical Analysis

We used Excel 2016 (Microsoft Corp.) and GraphPad Prism (version 7.0b for Mac OS; GraphPad Software, www.graphpad.com) for statistical analysis. Graphs were created with Sigmaplot 12 (Systat Software Inc.). We assessed the various PSMA SUV_{max} measurements with the Kruskal–Wallis-test, Mann–Whitney-test, Dunn's multiple-comparisons test, and Wilcoxon signed-rank test. A P value of less than 0.05 was considered statistically significant. To evaluate the SUV_{max} in different tissues and to generate a cutoff value to distinguish between normal intraprostatic tissue and malignant intraprostatic tissue, a receiver-operating characteristic analysis was used. The provided box plots show first and third quartile and median. The ends of the whiskers represent the 10th and 90th percentiles.

RESULTS

^{68}Ga-PSMA PET/CT was performed for 104 prostate cancer patients without previous local or systemic therapy. Mean SUV_{max} of gluteal muscle was 0.60 ± 0.10 for all prostate cancer patients. Healthy prostate tissue had a mean SUV_{max} of 1.88 ± 0.44 compared with 10.77 ± 8.45 for malignant intraprostatic lesions in corresponding patients ($P < 0.001$; Fig. 1). The mean SUV_{max} in all 104 patients was 14.47 ± 13.87. Forty-six patients (44.23%) showed unifocal uptake in the prostate. For 52 patients (50.00%), 2 or more loci with elevated SUV_{max} were observed; for 6 men (5.77%) the exact number of foci couldn't be determined. For 65 men (62.50%), only intraprostatic tracer uptake was detected. Of the prostate cancer patients undergoing PSMA PET/CT, 32.69% ($n = 34$) of patients were diagnosed with lymphatic metastases, 18.27% ($n = 19$) with bone metastases, and 11.54% ($n = 12$) with bone and lymphatic metastases (in total 38 bone metastases in 19 patients). Lymph node metastases were located within the pelvis for 17 patients (16.35%; Table 1). One patient with lung metastases and 1 patient with a penile metastasis were diagnosed. When PSMA PET/CT was compared with available MRI data, there was a match of detection of intraprostatic tumor lesions with highest available GS in 89.55%.

After correlation of intraprostatic, tumor-related tracer uptake with clinical parameters, a mean SUV_{max} of 8.55 ± 5.88 was detected in patients with current PSA values of less than 10 ng/mL compared with 14.97 ± 16.20 for PSA values of 10–20 ng/mL and 19.47 ± 15.47 for PSA values of more than 20 ng/mL ($P < 0.001$). When SUV_{max} and GS correlations were performed, prostate cancer lesions from biopsy with GS 6 and 7 had a mean SUV_{max} of 6.74 ± 6.10 and 11.06 ± 11.56, respectively (Fig. 2). The highest tracer uptake was found in intraprostatic lesions with a GS of 9, with a mean SUV_{max} of 22.16 ± 18.46. Prostate cancers with high GS (8–10) showed a statistically significant higher PSMA uptake (mean SUV_{max} of 19.61 ± 15.44) than tumors with a GS of 6 or 7 (mean SUV_{max} of 9.88 ± 10.49; $P < 0.001$). In ungrouped analyses, differences remained statistically significant for GS 6–10 as well as for grading system according to International Society of Urological Pathologists ($P < 0.001$ each; Fig. 3). Significant differences were also observed for risk classification based on the d'Amico scale (*22*): patients with high-risk tumors had higher intraprostatic PSMA uptake (mean SUV_{max} of 16.67 ± 14.88) compared with tumors with low (mean SUV_{max} of 5.97 ± 3.69) and intermediate risk (mean SUV_{max} of 6.98 ± 4.11) ($P < 0.001$; Table 2).

For subgroup analysis, correlations of intraprostatic SUV_{max} with clinical parameters were performed considering histopathologic data from surgery and biopsy type (MRI/TRUS-fusion biopsy). Comparison of clinical parameters with histologic results obtained only from MRI/TRUS-fusion biopsy also revealed statistically significant higher uptake in tumors with GS 8–10 than in those with GS 6–7 (mean SUV_{max}, 11.24 ± 12.9 and 19.45 ± 17.24, $P = 0.004$). From 28 men undergoing prostatectomy, mean SUV_{max} was 14.10 ± 11.07 ($n = 15$) for GS 7 tumors, compared with 20.41 ± 11.51 ($n = 13$) for GS 8–10 tumors (Fig. 4). This difference of intraprostatic tracer uptake was only of borderline significance ($P = 0.142$; Table 3). The correlation of histopathologic results from surgery with malignant, intraprostatic

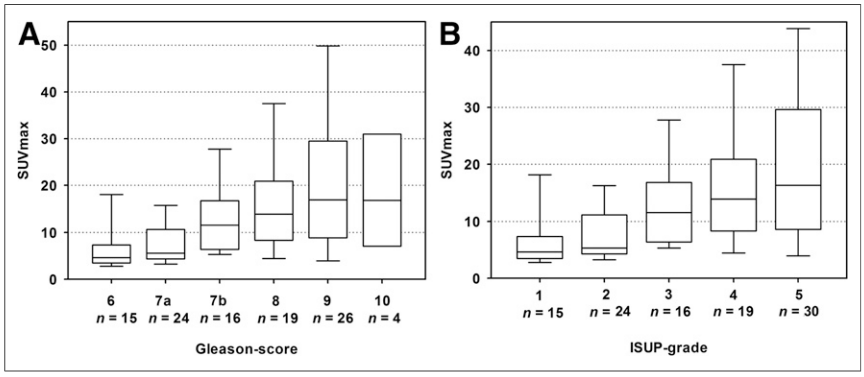

FIGURE 3. Box plot of SUV_{max} according to ungrouped GS in biopsy (A) and to International Society of Urologic Pathologists (ISUP) grade in biopsy (B).

TABLE 2
Comparison of SUV_{max} and Clinical Parameters

Clinical parameter	Median	Mean SUV_{max}	SD	*P*
Current PSA (n = 103)				<0.001
10	5.98	8.55	5.88	
10–20	7.94	14.97	16.20	
20	14.77	19.47	15.47	
GS in biopsy (grouped; n = 104)				<0.001
6–7	6.28	9.88	10.49	
8–10	16.29	19.61	15.44	
GS in biopsy (n = 104)				<0.001
6	4.62	6.74	6.10	
7a	5.56	9.74	13.47	
7b	11.56	13.04	7.89	
8	13.94	16.4	10.75	
9	16.99	22.16	18.46	
10	16.88	18.30	12.45	
d'Amico score (n = 104)				
Grouped				<0.001
Low/intermediate risk	5.79	6.72	3.95	
High risk	12.27	16.67	14.88	
Ungrouped				<0.001
Low risk	5.12	5.97	3.69	
Intermediate risk	5.79	6.98	4.11	
High risk	12.27	16.67	14.88	

lesions obtained from ^{68}Ga PSMA PET/CT leads to a calculated PET sensitivity and specificity of 68% and 92%, respectively. For PET/CT data correlating with MRI, there was a total or near-total match of increased tracer uptake in the same prostate segments in 91%.

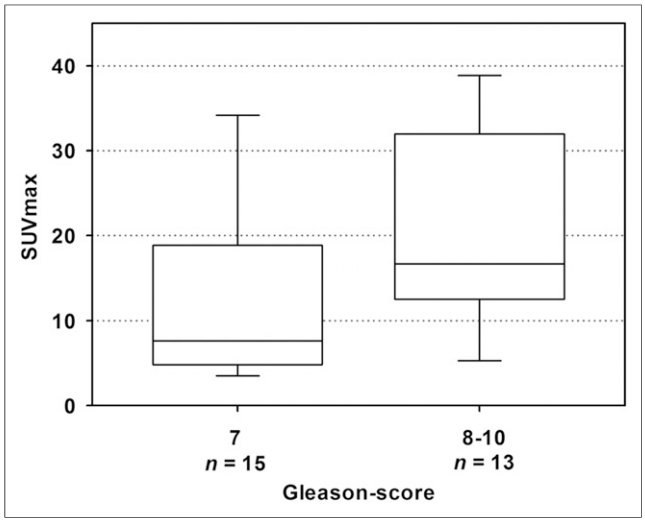

FIGURE 4. Box plot of SUV_{max} of GS (grouped) after prostatectomy.

TABLE 3
Comparison of SUV_{max} and GS in MR-Guided Biopsy and Prostatectomy

GS	Median	Mean SUV_{max}	SD	*P*
In MR-guided biopsy (grouped; n = 50)				0.004
7	7.59	11.24	12.9	
8–10	13.12	19.45	17.24	
After prostatectomy (grouped; n = 28)				0.14
7	8.32	14.1	11.07	
8–10	16.64	20.41	11.51	

DISCUSSION

To our knowledge, this is the largest study evaluating the role of ^{68}Ga-PSMA PET/CT as a primary staging tool for intraprostatic tumor lesions and the correlation with clinical and prognostic factors. Together with MRI and postsurgery histopathologic data as a reference test, we observed a statistically significant difference in mean SUV_{max} measurements between benign and malignant prostate tissue ($P < 0.001$). Intraprostatic lesions in 42 patients suspected of having a malignancy showed a mean SUV_{max} of 10.77 ± 8.45, which is comparable to other findings. The average SUV_{max} of histopathology-positive segments was 11.8 ± 7.6 in a recently published study of 21 patients with biopsy-proven prostate cancer (*23*). Fendler et al. reported on a mean SUV_{max} of 4.9 ± 2.9 for non-diseased segments (*23*) in comparison with 1.88 ± 0.44 in our study. Although a small cohort, a statistically significant difference was also observed for intraprostatic prostate cancer lesions and nonprostate cancer tissue in a group of 9 patients with histopathologically proven primary carcinoma of the prostate who underwent ^{68}Ga-PSMA PET/CT followed by radical prostatectomy (*24*). In receiver-operating-characteristic analyses (data not shown), an SUV_{max} cutoff of greater than 2.73 would lead to a sensitivity and specificity of 100% and 97.62% (95% confidence interval, 91.59%–100% and 87.43%–99.94%) in our cohort, respectively. These results need to be treated with caution because of the relatively small number of cases with histopathologic information and the arguable SUV measurements based on multiparametric MRI. Nevertheless, PSMA PET/CT seems to be a promising, diagnostic tool for the identification of malignant segments in the prostate.

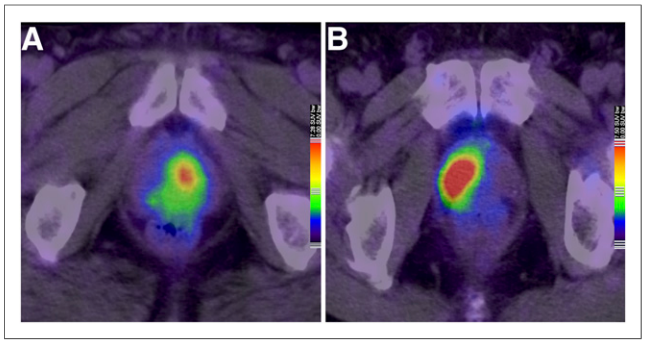

FIGURE 5. Different PSMA tracer uptake according to GS: 1 patient with GS 6 prostate cancer and SUV_{max} of 7.33 (A) compared with a GS 9 tumor and SUV_{max} of 16.64 (B).

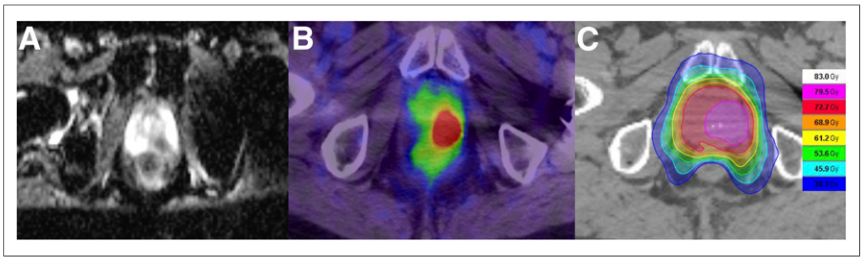

FIGURE 6. Relevant data for intraprostatic boost during radiotherapy: MRI of prostate with apparent diffusion coefficient sequence (A), PSMA tracer uptake in PSMA PET/CT (B), and radiation plan with irradiation of prostate and simultaneous integrated boost according to pretreatment imaging (C).

These findings are in accordance with results from 30 high-risk prostate cancer patients undergoing PSMA PET/CT imaging before radical prostatectomy. Budäus et al. reported that in 92.9% of patients, the intraprostatic tumor foci were predicted correctly (*25*). Therefore, PSMA PET/CT may play an important role not only in detecting metastases, but also in localizing tumor segments in the prostate. Similar to MRI-supported biopsy, cancer lesions can be traced with reference to PET imaging to avoid false-negative results or understaging of the tumor regarding the detection of the highest Gleason pattern. There might be a high potential to improve the current standard TRUS-biopsy in the same way as MRI. Lower rates of indolent cancer detection and a bigger proportion of identification of intermediate- and high-risk tumors using MRI/TRUS-fusion biopsy have already been described (*26*). Further studies are needed to evaluate the role of ^{68}Ga-PSMA PET/CT for prostate biopsy, also with regard to cost efficiency.

Furthermore, we investigated the correlation of intraprostatic PSMA uptake and several clinical parameters in subgroup analysis. Among a statistically significant difference of SUV_{max} regarding the present PSA, we also observed a significantly higher mean SUV_{max} in tumors with higher d'Amico risk classification and GS from biopsy ($P < 0.001$ for grouped analyses). In consideration of a small number of patients, these differences remained statistically significant ($P < 0.001$ each) in ungrouped evaluation (Fig. 5). There seems to be a strong trend of rising PSMA uptake with higher grade malignancy. To our knowledge, there is only 1 larger, recently published study apart from research using tissue microarrays that also described a correlation of tracer accumulation and clinical parameters: Uprimny et al. observed significantly lower PSMA uptake in tumors with GS 6–7b and PSA less than 10 ng/mL in a cohort of 90 men. The median SUV_{max} of intraprostatic, malignant lesions was 11.5 ng/mL compared with 3.9 ng/mL in normal prostate tissue (*17*). This relatively high SUV_{max} in healthy prostate tissue could be related to the fact that for calculation of SUV_{max} the tumor site was verified only by TRUS-guided biopsy, which has been proven insufficient (*6*). In contrast MRI/TRUS-fusion biopsy comprising targeted and systematic cores—which was done for nearly 50% of the patients in our cohort—leads to a precise definition of malignant and nonmalignant areas in the prostate (*27*). Uprimny et al. observed a lower SUV_{max} in GS 10 (17.7) than GS 9 (22.8) tumors (*17*)—in the same way as we did (GS 10, 18.3; GS 9, 22.2)—assuming that lower, intraprostatic tracer uptake is caused by dedifferentiation of tumor cells in GS 10 prostate carcinomas.

Another analysis performed by Fendler et al. observed a significantly lower SUV_{max} in histopathology-positive segments with GS of 6 compared with segments with GS of 7 or more with a P value of 0.012. However, no statistically significant difference was reported for segments with a GS of 7 or more (*23*). The relatively small-sized cohort ($n = 21$) and the small number of patients with a high GS (GS 8, 3 men; GS 9, 7 men) might explain the lack of difference compared with our findings.

Especially for definitive radiotherapy, identification of high malignant intraprostatic cancer segments is extremely helpful, because of the high risk for local recurrence of these so-called dominant intraprostatic tumor lesions after local treatment (*28,29*). The concept of treating dominant intraprostatic tumor lesions with an increased dose (boost) to improve local control is the objective of a currently recruiting randomized phase III trial (FLAME-trial), that is, however, based on an MRI-guided definition of dominant intraprostatic tumor lesions (*30*). It has recently been shown, that delineation of target volume and dominant intraprostatic tumor lesions is also feasible with PSMA PET/CT (*31*). Because of some benefits of PET compared with MRI, irradiation planning based on PSMA-PET/CT would be of great interest (Fig. 6).

The major limitations of our study are its retrospective nature and the small number of histopathologic results from prostatectomy. Most patients underwent radiotherapy or androgen deprivation after PSMA PET/CT, why validated, histopathologic data from surgery is only available for 26.92%. Further, some subgroups (e.g., high GS) only include a small number of patients. On the other hand, our study is one of the largest evaluating the role of PSMA PET/CT for intraprostatic tumor detection and correlation of SUV_{max} with GS and risk classification. Hence, our data can be used as a basis for further, prospective studies.

CONCLUSION

Our study confirms that PSMA PET/CT is an excellent diagnostic tool for the detection of intraprostatic tumor lesions. As one of the first analyses in a large patient cohort, our results indicate a correlation of tracer uptake with GS and d'Amico risk classification. This information might be useful for further diagnostic procedures, that is, biopsy-guidance and treatment planning in radiation oncology.

DISCLOSURE

This research was supported in part by the Klaus-Tschira-Stiftung (project no. 00.198.2012). No other potential conflict of interest relevant to this article was reported.

ACKNOWLEDGMENT

We express our sincere gratitude to Tim Holland-Letz for his excellent statistical assistance.

REFERENCES

1. Silver DA, Pellicer I, Fair WR, Heston WD, Cordon-Cardo C. Prostate-specific membrane antigen expression in normal and malignant human tissues. *Clin Cancer Res.* 1997;3:81–85.
2. Bostwick DG, Pacelli A, Blute M, Roche P, Murphy GP. Prostate specific membrane antigen expression in prostatic intraepithelial neoplasia and adenocarcinoma: a study of 184 cases. *Cancer.* 1998;82:2256–2261.

3. Afshar-Oromieh A, Malcher A, Eder M, et al. PET imaging with a [^{68}Ga]gallium-labelled PSMA ligand for the diagnosis of prostate cancer: biodistribution in humans and first evaluation of tumour lesions. *Eur J Nucl Med Mol Imaging.* 2013;40:486–495.
4. Afshar-Oromieh A, Zechmann CM, Malcher A, et al. Comparison of PET imaging with a ^{68}Ga-labelled PSMA ligand and ^{18}F-choline-based PET/CT for the diagnosis of recurrent prostate cancer. *Eur J Nucl Med Mol Imaging.* 2014;41:11–20.
5. Dietlein M, Kobe C, Kuhnert G, et al. Comparison of [^{18}F]DCFPyL and [^{68}Ga]Ga-PSMA-HBED-CC for PSMA-PET imaging in patients with relapsed prostate cancer. *Mol Imaging Biol.* 2015;17:575–584.
6. Ahmed HU, El-Shater Bosaily A, Brown LC, et al. Diagnostic accuracy of multiparametric MRI and TRUS biopsy in prostate cancer (PROMIS): a paired validating confirmatory study. *Lancet.* 2017;389:815–822.
7. Tonttila PP, Lantto J, Pääkkö E, et al. Prebiopsy multiparametric magnetic resonance imaging for prostate cancer diagnosis in biopsy-naive men with suspected prostate cancer based on elevated prostate-specific antigen values: results from a randomized prospective blinded controlled trial. *Eur Urol.* 2016; 69:419–425.
8. Maurer T, Gschwend JE, Rauscher I, et al. Diagnostic efficacy of ^{68}gallium-PSMA positron emission tomography compared to conventional imaging for lymph node staging of 130 consecutive patients with intermediate to high risk prostate cancer. *J Urol.* 2016;195:1436–1443.
9. Giesel FL, Sterzing F, Schlemmer HP, et al. Intra-individual comparison of ^{68}Ga-PSMA-11-PET/CT and multi-parametric MR for imaging of primary prostate cancer. *Eur J Nucl Med Mol Imaging.* 2016;43:1400–1406.
10. Bluemel C, Krebs M, Polat B, et al. ^{68}Ga-PSMA-PET/CT in patients with biochemical prostate cancer recurrence and negative ^{18}F-choline-PET/CT. *Clin Nucl Med.* 2016;41:515–521.
11. Shakespeare TP. Effect of prostate-specific membrane antigen positron emission tomography on the decision-making of radiation oncologists. *Radiat Oncol.* 2015;10:233.
12. Sterzing F, Kratochwil C, Fiedler H, et al. ^{68}Ga-PSMA-11 PET/CT: a new technique with high potential for the radiotherapeutic management of prostate cancer patients. *Eur J Nucl Med Mol Imaging.* 2016;43:34–41.
13. Dewes S, Schiller K, Sauter K, et al. Integration of ^{68}Ga-PSMA-PET imaging in planning of primary definitive radiotherapy in prostate cancer: a retrospective study. *Radiat Oncol.* 2016;11:73.
14. Minner S, Wittmer C, Graefen M, et al. High level PSMA expression is associated with early PSA recurrence in surgically treated prostate cancer. *Prostate.* 2011;71:281–288.
15. Kasperzyk JL, Finn SP, Flavin R, et al. Prostate-specific membrane antigen protein expression in tumor tissue and risk of lethal prostate cancer. *Cancer Epidemiol Biomarkers Prev.* 2013;22:2354–2363.
16. Perner S, Hofer MD, Kim R, et al. Prostate-specific membrane antigen expression as a predictor of prostate cancer progression. *Hum Pathol.* 2007;38:696–701.
17. Uprimny C, Kroiss AS, Decristoforo C, et al. ^{68}Ga-PSMA-11 PET/CT in primary staging of prostate cancer: PSA and Gleason score predict the intensity of tracer accumulation in the primary tumour. *Eur J Nucl Med Mol Imaging.* 2017;44:941–949.
18. Hope TA, Truillet C, Ehman EC, et al. ^{68}Ga-PSMA-11 PET imaging of response to androgen receptor inhibition: first human experience. *J Nucl Med.* 2017;58:81–84.
19. Meller B, Bremmer F, Sahlmann CO, et al. Alterations in androgen deprivation enhanced prostate-specific membrane antigen (PSMA) expression in prostate cancer cells as a target for diagnostics and therapy. *EJNMMI Res.* 2015;5:66.
20. Wright GL Jr, Grob BM, Haley C, et al. Upregulation of prostate-specific membrane antigen after androgen-deprivation therapy. *Urology.* 1996;48:326–334.
21. Eder M, Schäfer M, Bauder-Wüst U, et al. ^{68}Ga-complex lipophilicity and the targeting property of a urea-based PSMA inhibitor for PET imaging. *Bioconjug Chem.* 2012;23:688–697.
22. D'Amico AV, Whittington R, Malkowicz SB, et al. Biochemical outcome after radical prostatectomy, external beam radiation therapy, or interstitial radiation therapy for clinically localized prostate cancer. *JAMA.* 1998;280:969–974.
23. Fendler WP, Schmidt DF, Wenter V, et al. ^{68}Ga-PSMA PET/CT detects the location and extent of primary prostate cancer. *J Nucl Med.* 2016;57:1720–1725.
24. Zamboglou C, Schiller F, Fechter T, et al. ^{68}Ga-HBED-CC-PSMA PET/CT versus histopathology in primary localized prostate cancer: a voxel-wise comparison. *Theranostics.* 2016;6:1619–1628.
25. Budäus L, Leyh-Bannurah SR, Salomon G, et al. Initial experience of ^{68}Ga-PSMA PET/CT imaging in high-risk prostate cancer patients prior to radical prostatectomy. *Eur Urol.* 2016;69:393–396.
26. Siddiqui MM, Rais-Bahrami S, Turkbey B, et al. Comparison of MR/ultrasound fusion-guided biopsy with ultrasound-guided biopsy for the diagnosis of prostate cancer. *JAMA.* 2015;313:390–397.
27. Radtke JP, Schwab C, Wolf MB, et al. Multiparametric magnetic resonance imaging (MRI) and MRI-transrectal ultrasound fusion biopsy for index tumor detection: correlation with radical prostatectomy specimen. *Eur Urol.* 2016;70: 846–853.
28. Arrayeh E, Westphalen AC, Kurhanewicz J, et al. Does local recurrence of prostate cancer after radiation therapy occur at the site of primary tumor? Results of a longitudinal MRI and MRSI study. *Int J Radiat Oncol Biol Phys.* 2012;82: e787–e793.
29. Bott SR, Ahmed HU, Hindley RG, Abdul-Rahman A, Freeman A, Emberton M. The index lesion and focal therapy: an analysis of the pathological characteristics of prostate cancer. *BJU Int.* 2010;106:1607–1611.
30. Lips IM, van der Heide UA, Haustermans K, et al. Single blind randomized phase III trial to investigate the benefit of a focal lesion ablative microboost in prostate cancer (FLAME-trial): study protocol for a randomized controlled trial. *Trials.* 2011;12:255.
31. Zamboglou C, Wieser G, Hennies S, et al. MRI versus ^{68}Ga-PSMA PET/CT for gross tumour volume delineation in radiation treatment planning of primary prostate cancer. *Eur J Nucl Med Mol Imaging.* 2016;43:889–897.